

Observed Effects of Beam-Beam interactions on the Longitudinal Dynamics in the Tevatron

John Stogin Tanaji Sen
Princeton Fermilab

August 18, 2010

1 Introduction

The purpose of this paper is to understand if beam-beam effects have an impact on the longitudinal dynamics in the Tevatron. The Tevatron is a ring about 1km in diameter used for colliding a beam of protons with a beam of anti-protons (pbars). Each beam has 36 clusters (bunches) of particles. The general process is to inject the proton bunches and then the pbar bunches into the Tevatron at 150 GeV without any collisions taking place. During this time, the beam-beam interactions are simply the attractive forces seen between bunches as they travel by each other (in opposite directions). Each bunch experiences 72 of these interactions every time it travels around the Tevatron, because it passes by each of the 36 opposite bunches twice. After injection, the particles are accelerated to 980 GeV and the beams are made to collide at the center of the two experimental detectors (CDF and D0). At these spots, beam-beam interactions are head on collisions (of which there are 2 per revolution) and at other locations the same long-range interactions as those at 150 GeV (of which there are 70 per revolution).

Beam-beam interactions differ between proton and pbar bunches for a couple of reasons. First, since the proton bunches are injected first, they encounter an increasing number of pbar bunches as the pbar bunches are injected. The pbar bunches will always encounter proton bunches 72 times during one revolution. Also, proton bunches and pbar bunches vary in size and intensity. (This is mainly due to the fact that it is much harder to produce pbars than protons.) Although both proton bunches and pbar bunches have comparable brightness, the proton bunches are more intense and larger (in the transverse sense). Also, the pbar bunches tend to have more variation in intensity from bunch to bunch. See Figure 1 for a profile of a proton bunch and a pbar bunch. It should also be noted that the beam-beam interactions act as chromatic lenses. This means that they have differing effects on particles with different energies.

Particle bunches are centered about an ideal synchronous orbit in an “RF bucket” perfectly synchronized with the rf-cavity (the device that accelerates

the particles) in such a way that the orbit is a stable equilibrium. There are 1113 of these buckets in the Tevatron, and only 72 of these are used (36 for proton bunches and 36 for pbar bunches). Since the synchronous orbit is a stable equilibrium and no particle perfectly lies on this orbit, each particle in a bunch oscillates about the point that belongs to the ideal orbit. A good way to represent the state of a particle bunch is to plot its particle distribution in a plane with the horizontal axis being the time (resp. spatial) deviation from the ideal orbit and the vertical axis being the energy (resp. momentum) deviation from the ideal orbit. This plane is called phase space.

It is straightforward to measure the distribution of particles over some time interval, but it is not so clear how to obtain the energy distribution of these particles. To do so, we make use of the fact that the phase space distribution rotates slightly each time the bunch completes a turn in the Tevatron. Letting ΔE_n denote the energy offset of a particle at the n th turn and ϕ_n denote the phase offset of the particle relative to the synchronous orbit, we have the recursion relations:[2]

$$\phi_{n+1} = \phi_n + \frac{\omega_{rf}\tau\eta c^2}{v^2 E_s} \Delta E_{n+1}$$

$$\Delta E_{n+1} = \Delta E_n + eV \sin \phi_n$$

(In the previous relations, ω_{rf} is the RF cavity frequency, τ is the revolution period, η is the slip factor, c is the speed of light, v is the velocity of the particle, E_s is the operating energy of the ideal orbit, and eV is the product of the charge of a proton and the maximum voltage of the RF cavity.) This relation is used by the phase space reconstruction program, but for now, what is important is not really the actual recursion relation, but the fact that it corresponds to a rotation of phase space.

Measuring the time distribution of particles over a number of turns is equivalent to measuring the projection of the phase space distribution in many different directions. The same principle is used in tomographic reconstructions done with CAT scans and MRI scans. Having these measurements, it is possible to reconstruct the entire phase space. The actual code used to do this was obtained from CERN. [1]

2 The Data

The data was collected from a resistive wall monitor placed inside the Tevatron. A moving bunch of particles induces a current on the wall proportional to the number of particles. The wall monitor is a gap in the wall with resistors placed across it so that the current traveling through the resistors provides a measurable voltage. This voltage is recorded to produce a profile of the bunch in time. Figure 1 shows a graphical representation of part of the data that was collected. It shows a proton bunch on the left and an anti-proton (or pbar) bunch on the right. The entire data set contains 12 of each of these bunches. The multiple

curves correspond to multiple recordings of the bunch while it passes by the wall monitor. In other words, the data set shows how the bunches evolve as they travel around the Tevatron ring an integer number of turns. The entire data set consists of 128 of these observed turns.

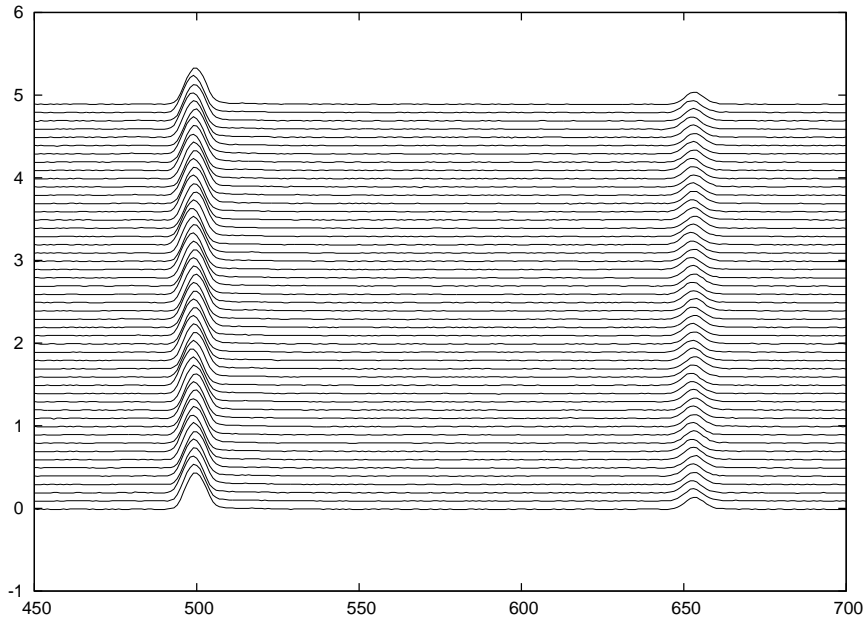


Figure 1: Part of the data captured from the wall monitor. On the left is a Proton bunch and on the right is a Pbar bunch. The entire data set contains 12 of each of these.

The data was captured at seven different stages. The first three occur at 150 GeV and the last four occur at 980 GeV. The stages are listed below:

- Stage 1** After the first four pbar bunches for each train have been injected and cogged.
- Stage 2** After the first eight pbar bunches for each train have been injected and cogged.
- Stage 3** After all pbar bunches have been injected and cogged. (Just before acceleration)
- Stage 4** After acceleration to 980 GeV and final cogging.
- Stage 5** During initial collisions.
- Stage 6** Beginning of High Energy Physics (called HEP. This is the start of data capture).

Stage 7 1 hour and 47 minutes after Stage 6.

The data was captured at a rate of 1Gs/sec. For the 150 GeV stages, a turn was recorded once every 6 actual turns around the Tevatron, and for 980 GeV stages, a turn was recorded once every 11 actual turns around the Tevatron.

3 Phase Space

Phase space plots were generated using the tomography code for each bunch at every stage to look for shapes indicative of higher order modes or unexpected consequences of nonlinear forces. A few things were observed: (1) The phase space during the 150 GeV stages is less concentrated, because the bunch is larger. (2) During the initial collisions and beginning of HEP, the phase spaces exhibit a slight triangular shape, which indicates a higher order mode. These observations may be seen for various bunches in Appendix A.

A few of these phase space plots, when originally generated, had extra points which do not seem to actually belong to the phase space. (See Figure 2) The phase space plots are represented by a 19*19 grid of doubles, but appear more precise due to the graphics rendering. The isolated regions in the left plot of Figure 2 are represented by a single nonzero double. We do not think they actually belong to the phase space since they are isolated and in some cases can be extreme compared to the rest of the phase space. They are unwanted, because they distort the shape of the phase space and influence the color scheme of the plots.

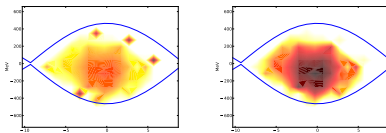


Figure 2: Phase space plots of bunch 0 at the second stage before and after applying filtering

To circumvent this problem, we employed a simple filtering scheme. For each point in the 17*17 grid centered in the 19*19 grid, the average of the eight surrounding points is computed. If the value of the given point exceeds four times that average, its value is replaced by that average. Figure 2 shows a sample phase space plot before and after applying this filtering technique. Unfortunately, we do not expect to have removed all of these outliers, and we suspect that the plot for the third stage seen in Figure 12 (for example) still contains at least one of these points, which makes the phase space appear slightly lighter than the first two.

The phase space plots were also used to obtain a momentum distribution by projecting the phase space on the momentum axis for each bunch at each stage. Appendix B contains mountain range plots for a few of these bunches.

We expect the distribution to have a Gaussian profile but that is not always the case. A sample plot is shown in Figure 3. For each of these profiles, the value $\frac{\langle \frac{\Delta P}{P}^4 \rangle}{3\langle \frac{\Delta P}{P}^2 \rangle^2}$ was calculated and plotted in Figure 4. This value is a measure for how well the momentum profile resembles a Gaussian distribution (1 = perfect Gaussian). One can see that the momentum profiles mostly resemble Gaussian distributions at 980 GeV around the start of collisions.

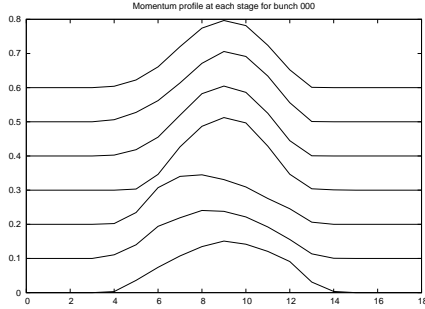


Figure 3: The momentum profile for proton bunch 0 at each stage. Similar plots for other bunches may be seen in Appendix B.

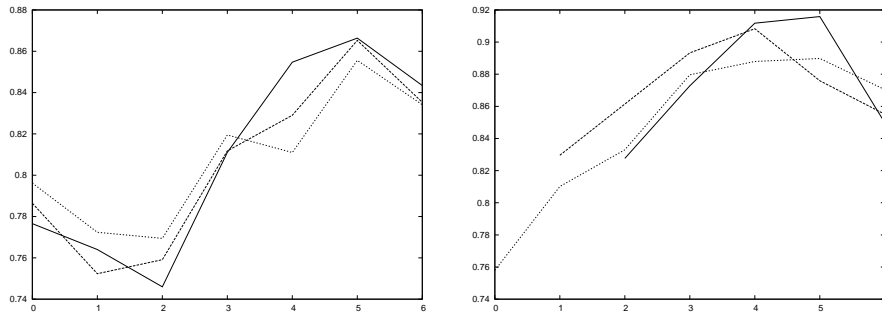


Figure 4: A measure of how well the momentum distribution at each stage resembles a Gaussian (1 = perfect Gaussian) for proton bunches 0,5,11 (left) and pbar bunches 0,5,10 (right).

In Figure 4, one can see that the presence of pbar bunches has the effect of increasing the tails of the distribution and decreasing the Gaussian resemblance of the momentum distributions of proton bunches. This is an effect of the long-range beam-beam forces.

4 Bunch Area

To quantify the area of the phase space plots, projections were taken onto both the horizontal ϕ and vertical $\Delta P/P = \Delta E/E_s$ axes. From those distributions,

the RMS width (σ_ϕ and $\sigma_{\Delta P/P}$) were calculated. The product of these two standard deviations is a measure of area and its evolution over the stages at 980 GeV are shown in Figure 5.

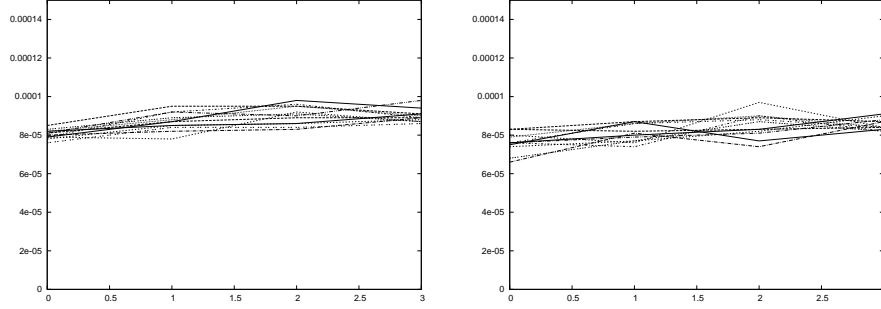


Figure 5: A plot of the evolution in $\sigma_\phi\sigma_{\Delta P/P}$ across stages at 980 GeV for protons (left) and pbars (right)

From these plots, a slight increasing trend may be observed, but it is not significant when compared to the variation among bunches.

5 Particle Loss

Bunches were also analyzed to see how many particles were lost between stages at 980 GeV. The area under the measured longitudinal distributions (seen for example in Figure 1) is a measure of the bunch intensity. The fraction of particle loss is illustrated in Figure 6. It can be seen that between the first couple of stages, roughly 1–2% of particles are lost and that over 1hr 47mins of colliding, about 6–7% of protons are lost with one bunch losing over 10%. Pbars bunches seem to lose particles about twice as quickly as the proton bunches do.

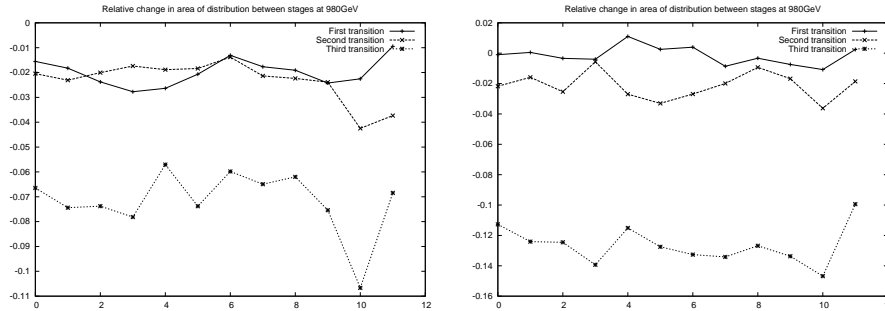


Figure 6: Fraction of particle loss between stages at 980 GeV for proton bunches (left) and pbar bunches (right)

6 Bunch Position

An analysis was performed on the bunch position by calculating the center of the distribution and taking a Fast Fourier Transform over the resulting 128 observed turns at each stage. When computing a Fast Fourier Transform on data containing points separated by time interval Δt , the range of the frequency spectrum is $1/(2\Delta t)$. Since each observed turn occurred every 6 turns at 150 GeV stages and every 11 turns at 980 GeV stages, the frequency range of the Fast Fourier Transform is $1/(2*6*22\mu s) \approx 3800\text{hz}$ and $1/(2*11*22\mu s) \approx 2100\text{hz}$ at these respective energy levels. The FFT resolution is $1/(N\Delta t)$, where N is the number of samples (128 in this case). This means the respective resolutions are $3800\text{hz}/64 \approx 60\text{hz}$ and $2100\text{hz}/64 \approx 33\text{hz}$.

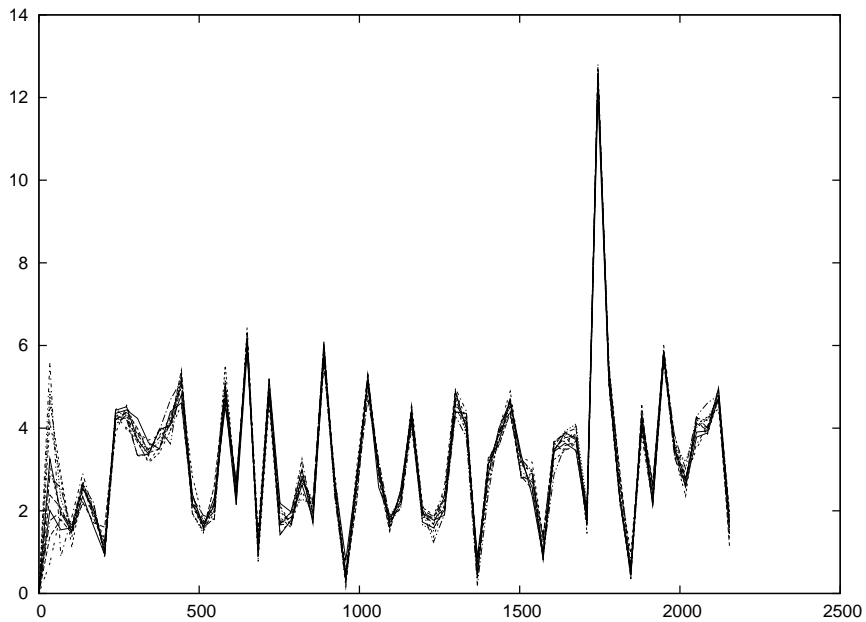


Figure 7: The Fourier spectrum of all 12 proton bunches just after reaching 980 GeV

It is possible to see from Figure 7 that the Fourier spectrum is almost the same for each of the 12 proton bunches. There is a little more variation amongst the pbar bunches. This is representative of all 7 stages. The Fourier spectrum changes at different stages. The stage by stage evolution is shown in Figure 8.

It is worth noting that for every bunch, the dominant frequency at 150 GeV is 3322hz and for the first three stages at 980 GeV is 1744hz . Between the third and fourth stages (corresponding to an elapsed time of roughly 1hr 47mins) at 980 GeV, the dominant frequency drops by one resolution unit to 1710hz . It is also worth noting that the spike at the dominant frequency seems to widen at the start of initial collisions.

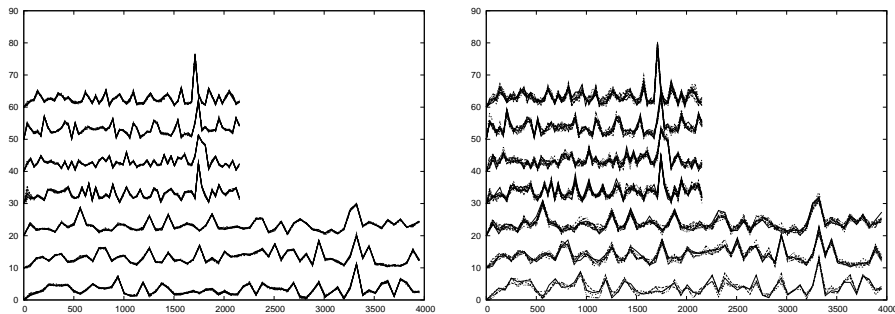


Figure 8: The Fourier spectrum of proton (left) and pbar (right) bunches over all seven stages, starting with the first stage shown at the bottom and progressing upwards. The fourth stage in the proton plot is the same as the plot in Figure 7

Some analysis was done to determine if any of the peaks seem to match integer multiples of some base frequency. In particular, we looked for peaks at integer multiples of 60hz (the operating frequency of the power grid) and found that a number of peaks match up with odd integer multiples of 60hz in the first 980 GeV stage. This can be seen in Figure 9. Another analysis looks at the difference in frequencies between peaks. We define a peak to be a frequency with FFT amplitude > 4.5 and then plot at each peak value the difference in frequency between that and the previous peak. The plot is shown in Figure 10. A horizontal trend among the points indicates a possible base frequency which shows up in higher order harmonics. We observe there are several peaks with a difference of 168Hz.

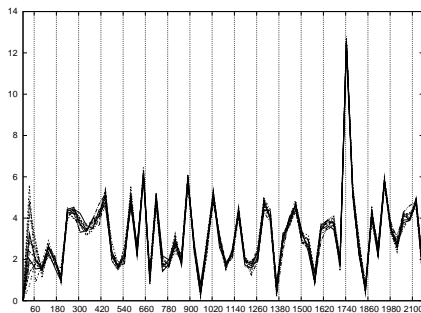


Figure 9: Figure 7 with lines plotted at odd integer multiples of 60hz. Keep in mind that the resolution (34hz) is about a quarter of the distance between lines.

Similar analyses were also performed on higher order moments of the time distribution, but there were no significant observations. For example, the second

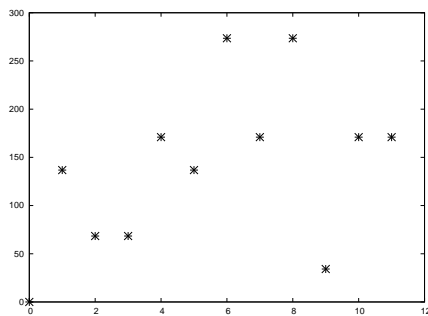


Figure 10: Difference in frequency between peaks shown in Figure 7. A horizontal line is a correlation possibly indicating a base frequency.

moment (standard deviation), shown in Figure 11 saw little consistency among the bunches. This implies there is much greater variation in 2nd and higher order modes from bunch to bunch. This plot should be compared with Figure 7, which is a plot of the first moment.

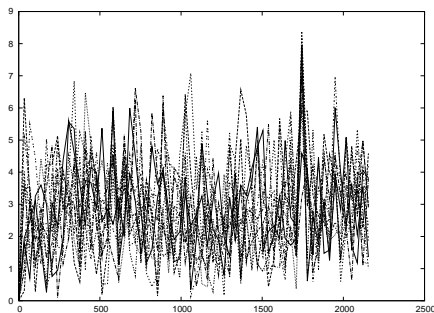


Figure 11: A FFT of the standard deviation of all 12 proton bunches just after reaching 980 GeV. This should be compared to Figure 7.

7 Conclusion

The findings may be summarized as follows:

- The phase space plots do not reveal anything unusual, but it would be nice to have a better resolution.
- The presence of pbar bunches in the Tevatron seems to change the momentum distributions of the proton bunches so that they are less Gaussian in shape.
- The bunch area corresponding to the phase space is smaller at 980 GeV as expected, but it does not significantly increase over time during collisions.
- After colliding for 1hr 47mins, proton bunches lose about 7% of particles and pbar bunches lose about 12%.
- A bunch that loses significantly more particles over time shows signs of heavy loss in the beginning of collisions.
- Bunch spectra have the largest peaks at 3322hz at 150 GeV and 1744hz at 980 GeV. The peak at this frequency widens during initial collisions and the frequency decreases over time.

It would be helpful to improve data accuracy in the future by increasing the sampling rate and recording more turns. For example, the scope used has the capability of measuring data at 2 Gs/sec (although only 64 turns could be recorded in this case). There is another scope, which was unavailable at the time of data collection, that can record 8000 turns. By recording data over 4096 turns, we could get a precision of $3800hz/2048 \approx 1.9hz$ at 150 GeV and $2100hz/2048 \approx 1hz$. Another way of changing the resolution is to change the number of turns between successive recordings. Recording twice as frequently would result in a doubly precise FFT, but would require twice the memory to observe an entire synchrotron period. It would also be useful to perform a similar analysis on multiple stores to see whether these findings are consistent.

A Reconstructed Phase Space Plots

These are phase space plots obtained by using the phase space reconstruction code.[1] The first three plots are at 150 GeV stages and the last four are at 980 GeV stages. Some pbar bunches may be missing plots, since they had not yet been inserted into the Tevatron.

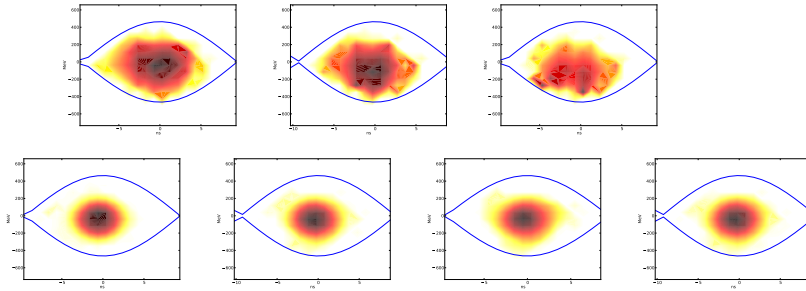


Figure 12: Proton bunch 0

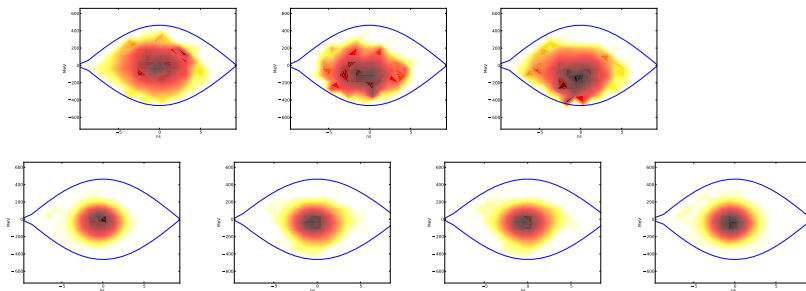


Figure 13: Proton bunch 5

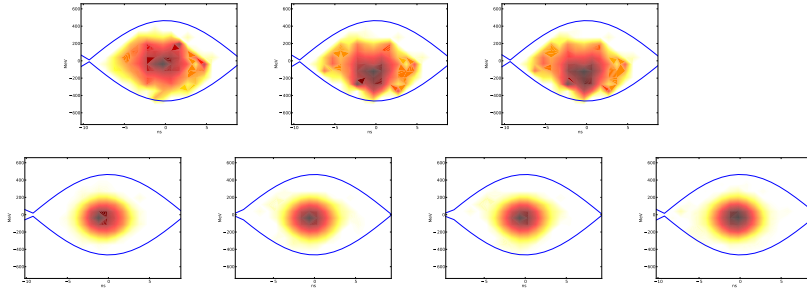


Figure 14: Proton bunch 11

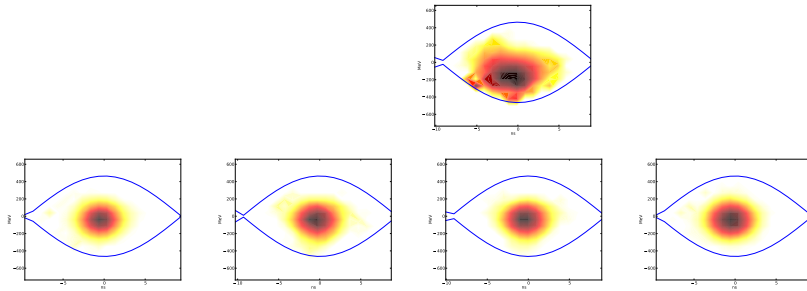


Figure 15: Pbar bunch 0

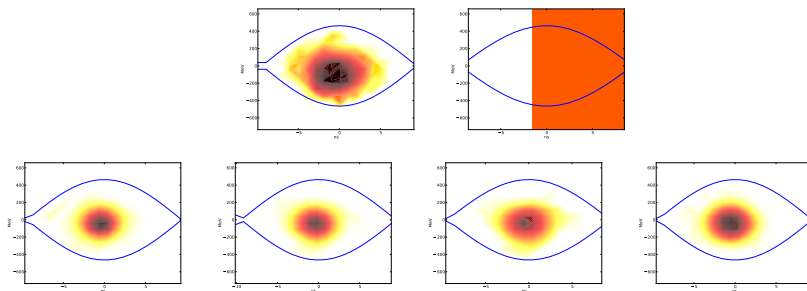


Figure 16: Pbar bunch 5 (There was a problem with generating the plot for the third stage. A possible explanation is that the oscilloscope did not trigger properly when capturing data)

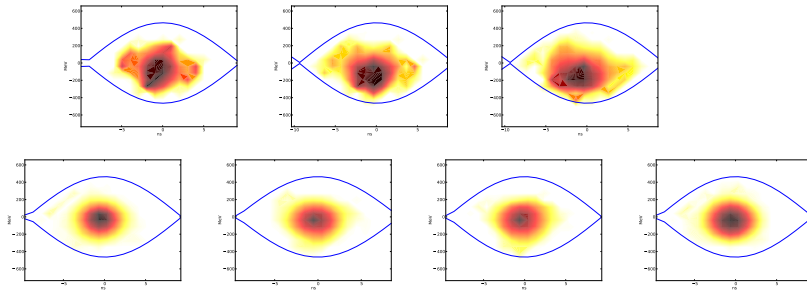


Figure 17: Pbar bunch 10

B Momentum Distribution Mountain Range Plots

These are mountain range plots of the momentum distributions obtained by projecting the phase space distributions onto the momentum (vertical) axis. A distribution is given at each energy stage with the first stage appearing on the bottom.

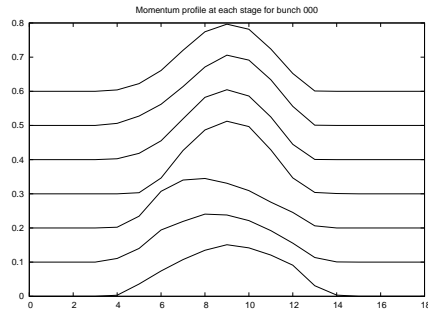


Figure 18: Proton bunch 0

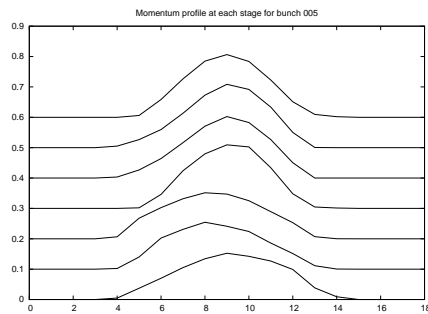


Figure 19: Proton bunch 5

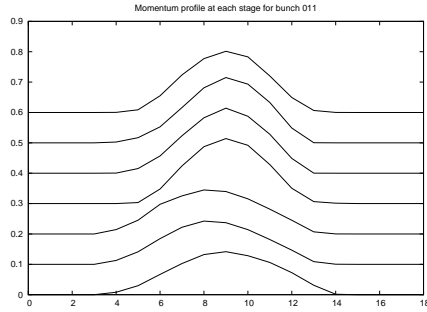


Figure 20: Proton bunch 11

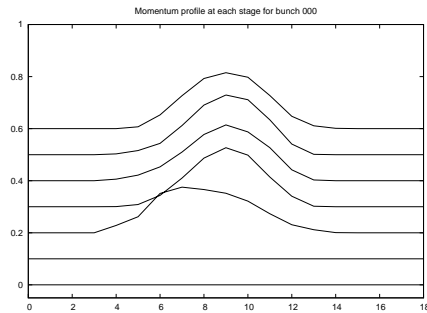


Figure 21: Pbar bunch 0

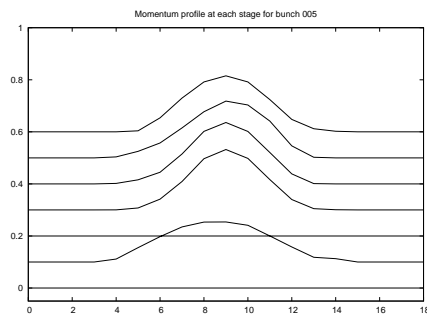


Figure 22: Pbar bunch 5. There was a problem during reconstruction of the third stage. (See Figure 16)

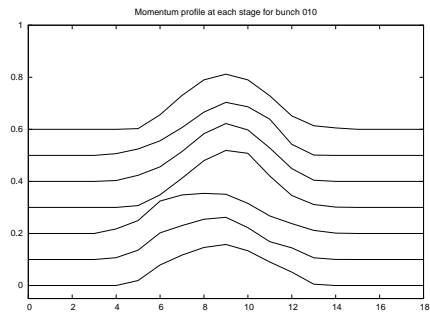


Figure 23: Pbar bunch 10

References

- [1] <http://tomograp.web.cern.ch/tomograp/>
- [2] Edwards, D., and M. Syphers. *An Introduction to the Physics of High Energy Accelerators*. New York: Wiley, 1993.